A Discontinuous Galerkin method with weighted averages for advection-diffusion equations with locally small and anisotropic diffusivity

Alexandre Ern[*]   Annette F. Stephansen[†]   Paolo Zunino[‡]

November 29, 2007

Abstract

We propose and analyze a symmetric weighted interior penalty (SWIP) method to approximate in a Discontinuous Galerkin framework advection-diffusion equations with anisotropic and discontinuous diffusivity. The originality of the method consists in the use of diffusivity-dependent weighted averages to better cope with locally small diffusivity (or equivalently with locally high Péclet numbers) on fitted meshes. The analysis yields convergence results for the natural energy norm that are optimal with respect to mesh-size and robust with respect to diffusivity. The convergence results for the advective derivative are optimal with respect to mesh-size and robust for isotropic diffusivity, as well as for anisotropic diffusivity if the cell Péclet numbers evaluated with the largest eigenvalue of the diffusivity tensor are large enough. Numerical results are presented to illustrate the performance of the proposed scheme. discontinuous Galerkin, weighted averages, locally small diffusion with advection, anisotropic diffusion

1 Introduction

Since their introduction over thirty years ago [19, 16], Discontinuous Galerkin (DG) methods have emerged as an attractive tool to approximate numerous PDEs in the engineering sciences. Here we are primarily interested in advection–diffusion equations with anisotropic (e.g., tensor-valued) and heterogeneous (e.g., non-smooth) diffusivity. Such equations are encountered, for instance, in groundwater flow models which constitute the motivation for the present work.

The analysis of DG methods to approximate advection–diffusion equations is extensively covered in [15]. This work already addresses anisotropic and heterogeneous diffusivity. However, one particular aspect that deserves further attention is that where the diffusivity becomes very small in *some* parts of the computational domain. Indeed, in this case it is well-known that the presence of an advective field can trigger internal layers. In the locally vanishing diffusivity limit, the solution becomes discontinuous on the interfaces where the advective field flows from the vanishing-diffusivity

---

[*]Université Paris-Est, CERMICS, Ecole des Ponts ParisTech, 77455 Marne la Vallée cedex 2, France (`ern@cermics.enpc.fr`).

[†]Andra, Parc de la Croix-Blanche, 1-7 rue Jean Monnet, 92298 Châtenay-Malabry cedex, France.

[‡]MOX, Dipartimento di Matematica "F. Brioschi", Politecnico di Milano, via Bonardi 9, 20133 Milano, Italy.

region towards the nonvanishing-diffusivity region. This situation has been analyzed in [10] and, more recently, in [5, 6]. For (very) small but positive diffusivity, the usual DG methods meet with difficulties in the presence of internal layers that are not sufficiently resolved by the mesh. Indeed, these methods are designed to weakly enforce continuity of the discrete solution across mesh interfaces, but because internal layers are under-resolved, the exact solution is better approximated by a discontinuous function at the interfaces adjacent to internal layers. One possible remedy is to consider a hard-wired modification of the DG method at those interfaces, as already proposed in [15] and, more recently, in [8]. However, a more satisfactory approach would be to design a DG method that can handle internal layers in an automated fashion. This is the purpose of the present work. The key ingredient is the use of weighted instead of arithmetic averages in certain interface terms of the DG method, with weights depending on the diffusivity on both sides of the interface. The present method relies on the (mild) assumption that fitted meshes are used, i.e., that discontinuities in the diffusivity are aligned with the mesh. When this assumption is not possible (e.g., in the case of nonlinear diffusivity), the present method is not expected to behave better than the usual DG methods, since all methods will suffer from the fact that they attempt to approximate a rough solution within some mesh elements.

The idea of utilizing weighted averages stems from the mortar finite-element method originally proposed by Nitsche [17, 18]. This method imposes weakly the continuity of fluxes between different regions. Various authors have highlighted the possibility of using an average with weights that differ from one half; see [21, 14, 12, 13] where several mortaring techniques are presented to match conforming finite elements on possibly nonconforming computational meshes. In the cited works, weighted averages are introduced as a generalization of standard averages and the analysis is carried out in the general framework, but a possible dependency of the weights on the coefficients of the problem is not considered. This dependency was investigated recently in [3] for isotropic advection–diffusion problems, using a weighted interior penalty technique with mortars; when applied elementwise, this approach yields a DG method. It was shown in [3] that a specific choice of weights improves the stability of the scheme when the diffusivity takes locally small values. The reason why weighted averages are needed to properly handle internal layers is rooted in the dissipative structure of the underlying Friedrichs's system. The design of the corresponding DG bilinear form, where dissipation at the discrete level is enforced by a consistency term involving averages, has been recently proposed in [7]. The extension to advection–diffusion equations including the locally vanishing diffusivity limit is analyzed in [6].

In the present work, we extend the DG method implicitly derived in [3] for isotropic diffusivity to anisotropic problems. This task is not as simple as it may appear on first sight since the presence of internal layers now depends on the spectral structure of the diffusivity tensor on both sides of each mesh interface. The spectral structure also raises the question of the appropriate choice of the penalty term in the DG method at each mesh interface. The analysis presented below will tackle these issues.

We design and analyze one specific DG method with weighted averages, namely the Symmetric Weighted Interior Penalty (SWIP) method, obtained by modifying the well-known (Symmetric) Interior Penalty (IP) method [2, 1]. Many other well-known DG methods, including the Local Discontinuous Galerkin method [4] and the Nonsymmetric Interior Penalty Galerkin method [20], can also be modified to fit the present scope; for brevity, these developments are omitted herein.

This paper is organized as follows: Section 2 presents the setting under scrutiny and formulates the SWIP method, while Section 3 contains the error analysis in the natural

energy norm for the problem. The estimate is fully robust, meaning that the constant in the error upper bound is independent of both heterogeneities and anisotropies in the diffusivity. Section 4 is concerned with the error analysis on the advective derivative. The derived estimate is again robust with respect to heterogeneities in the diffusivity, but the constant in the error upper bound can in some cases depend on local anisotropies. Robustness is achieved for instance if the cell Péclet numbers evaluated with the largest eigenvalue of the diffusivity tensor are large enough. Numerical results, including comparisons with the more usual IP methods, are presented in Section 5 and illustrate the benefits of using weighted interior penalties to approximate advection–diffusion equations with locally small and anisotropic diffusivity. Finally, Section 6 contains some concluding remarks.

2 The SWIP method

Let Ω be a domain in $\mathbb{R}^d$ with boundary $\partial\Omega$ in space dimension $d \in \{2,3\}$. We consider the following advection-diffusion equation with homogeneous Dirichlet boundary conditions:

$$\begin{cases} -\nabla\cdot(K\nabla u) + \beta\cdot\nabla u + \mu u = f & \text{in } \Omega, \\ u = 0 & \text{on } \partial\Omega. \end{cases} \tag{1}$$

Here $\mu \in L^\infty(\Omega)$, $\beta \in [W^{1,\infty}(\Omega)]^d$, the diffusivity tensor K is a symmetric, positive definite field in $[L^\infty(\Omega)]^{d,d}$ and $f \in L^2(\Omega)$. The regularity assumption on β can be relaxed, but is sufficient for the present purpose. The weak formulation of (1) consists of finding $u \in H_0^1(\Omega)$ such that

$$(K\nabla u, \nabla v)_{0,\Omega} + (\beta\cdot\nabla u, v)_{0,\Omega} + (\mu u, v)_{0,\Omega} = (f,v)_{0,\Omega} \quad \forall v \in H_0^1(\Omega) \tag{2}$$

where $(\cdot,\cdot)_{0,\Omega}$ denotes the L^2-scalar product on Ω. Henceforth, we assume that

$$\mu - \tfrac{1}{2}\nabla\cdot\beta \geq \mu_0 > 0 \qquad \text{a.e in } \Omega. \tag{3}$$

Furthermore, we assume that the smallest eigenvalue of K is bounded from below by a positive (but possibly very small) constant. Then, owing to the Lax–Milgram Lemma, (2) is well–posed.

Let $\{\mathscr{T}_h\}_{h>0}$ be a shape-regular family of affine triangulations of the domain Ω. The meshes $\mathscr{T}_h$ may possess hanging nodes. For simplicity we assume that the meshes cover Ω exactly, i.e., Ω is a polyhedron. A generic element in $\mathscr{T}_h$ is denoted by T, h_T denotes the diameter of T and n_T its outward unit normal. Set $h = \max_{T \in \mathscr{T}_h} h_T$. We assume without loss of generality that $h \leq 1$. Let $p \geq 1$. We define the classical DG approximation space

$$V_h = \{v_h \in L^2(\Omega); \forall T \in \mathscr{T}_h, v_h|_T \in \mathbb{P}_p\}, \tag{4}$$

where $\mathbb{P}_p$ is the set of polynomials of total degree less than or equal to p. Henceforth, we assume that the discontinuities in the diffusivity tensor are aligned with the mesh. This is a mild assumption in the context of linear problems. Moreover, for the sake of simplicity, we assume that the diffusivity tensor K is piecewise constant on $\mathscr{T}_h$. This assumption, which is reasonable in the context of groundwater flow models, can be generalized by assuming a smooth enough behavior of K inside each mesh element.

3

We say that F is an interior face of the mesh if there are $T^-(F)$ and $T^+(F)$ in $\mathscr{T}_h$ such that $F = T^-(F) \cap T^+(F)$. We set $\mathscr{T}(F) = \{T^-(F), T^+(F)\}$ and let n_F be the unit normal vector to F pointing from $T^-(F)$ towards $T^+(F)$. The analysis hereafter does not depend on the arbitrariness of this choice. Similarly, we say that F is a boundary face of the mesh if there is $T(F) \in \mathscr{T}_h$ such that $F = T(F) \cap \partial\Omega$. We set $\mathscr{T}(F) = \{T(F)\}$ and let n_F coincide with the outward normal to $\partial\Omega$. All the interior (resp., boundary) faces of the mesh are collected into the set $\mathscr{F}_h^i$ (resp., $\mathscr{F}_h^{\partial\Omega}$) and we let $\mathscr{F}_h = \mathscr{F}_h^i \cup \mathscr{F}_h^{\partial\Omega}$. Henceforth, we shall often deal with functions that are double-valued on $\mathscr{F}_h^i$ and single-valued on $\mathscr{F}_h^{\partial\Omega}$. This is the case, for instance, of functions in V_h. On interior faces, when the two branches of the function in question, say v, are associated with restrictions to the neighboring elements $T^\mp(F)$, these branches are denoted by $v^\mp$ and the jump of v across F is defined as

$$[\![v]\!]_F = v^- - v^+. \tag{5}$$

On a boundary face $F \in \mathscr{F}^{\partial\Omega}$, we set $[\![v]\!]_F = v|_F$. Furthermore, on an interior face $F \in \mathscr{F}_h^i$, we define the standard (arithmetic) average as $\{v\}_F = \frac{1}{2}(v^- + v^+)$. The subscript F in the above jumps and averages is omitted if there is no ambiguity.

The L^2-scalar product and its associated norm on a subset $R \subset \Omega$ (evaluated with the appropriate Lebesgue's measure) are indicated by the subscript $0, R$. For $s \geq 1$, a norm (seminorm) with the subscript s, R designates the usual norm (seminorm) in $H^s(R)$. When the region R is the boundary of a mesh element ∂T and the arguments in the scalar product or the norm are double-valued functions, it is implicitly assumed that the value considered is that of the branch associated with the restriction to T. For $s \geq 1$, $H^s(\mathscr{T}_h)$ denotes the usual broken Sobolev space on $\mathscr{T}_h$ and for $v \in H^1(\mathscr{T}_h)$, $\nabla_h v$ denotes the piecewise gradient of v, that is, $\nabla_h v \in [L^2(\Omega)]^d$ and for all $T \in \mathscr{T}_h$, $(\nabla_h v)|_T = \nabla(v|_T)$. It is also convenient to set $V(h) = H^2(\mathscr{T}_h) + V_h$.

The formulation of the SWIP method requires two parameters. As in the formulation of the usual IP method we introduce a single- and scalar-valued function γ defined on $\mathscr{F}_h$. The purpose of this function is to penalize jumps across interior faces and values at boundary faces. Additionally, we define a scalar- and double-valued function ω on $\mathscr{F}_h^i$. This function, which is not present in the usual IP method, is used to evaluate weighted averages of diffusive fluxes. On an interior face $F \in \mathscr{F}_h^i$, the values taken by the two branches of ω are denoted by $(\omega|_F)^\mp$, or simply $\omega^\mp$ if there is no ambiguity. Henceforth, it is assumed that for all $F \in \mathscr{F}_h^i$, both values are non-negative and that

$$\omega^- + \omega^+ = 1. \tag{6}$$

For $v \in V(h)$, we define the weighted average of the diffusive flux $K\nabla_h v$ on an interior face $F \in \mathscr{F}_h^i$ as

$$\{K\nabla_h v\}_\omega = \omega^-(K\nabla_h v)^- + \omega^+(K\nabla_h v)^+. \tag{7}$$

For convenience, we extend the above definitions to boundary faces as follows: on $F \in \mathscr{F}_h^{\partial\Omega}$, ω is single-valued and equal to 1, and we set $\{K\nabla v\}_\omega = K\nabla v$.

The SWIP bilinear form $B_h(\cdot, \cdot)$ is defined on $V(h) \times V(h)$ as follows

$$\begin{aligned}
B_h(v, w) = {} & (K\nabla_h v, \nabla_h w)_{0,\Omega} + ((\mu - \nabla\cdot\beta)v, w)_{0,\Omega} - (v, \beta\cdot\nabla_h w)_{0,\Omega} \\
& + \sum_{F \in \mathscr{F}_h} \left((\gamma[\![v]\!], [\![w]\!])_{0,F} - (n_F^t\{K\nabla_h v\}_\omega, [\![w]\!])_{0,F} - (n_F^t\{K\nabla_h w\}_\omega, [\![v]\!])_{0,F} \right) \\
& + \sum_{F \in \mathscr{F}_h^i} (\beta\cdot n_F\{v\}, [\![w]\!])_{0,F} + \sum_{F \in \mathscr{F}_h^{\partial\Omega}} \tfrac{1}{2}(\beta\cdot n_F v, w)_{0,F}.
\end{aligned} \tag{8}$$

4

The SWIP bilinear form can equivalently be expressed, after integrating the advective derivative by parts, as

$$B_h(v,w) = (K\nabla_h v, \nabla_h w)_{0,\Omega} + (\mu v, w)_{0,\Omega} + (\beta \cdot \nabla_h v, w)_{0,\Omega}$$
$$+ \sum_{F \in \mathscr{F}_h} \left((\gamma[\![v]\!], [\![w]\!])_{0,F} - (n_F^t \{K\nabla_h v\}_\omega, [\![w]\!])_{0,F} - (n_F^t \{K\nabla_h w\}_\omega, [\![v]\!])_{0,F} \right)$$
$$- \sum_{F \in \mathscr{F}_h^i} (\beta \cdot n_F \{w\}, [\![v]\!])_{0,F} - \sum_{F \in \mathscr{F}_h^{\partial\Omega}} \tfrac{1}{2} (\beta \cdot n_F v, w)_{0,F}. \tag{9}$$

Both (8) and (9) will be used in the analysis. The discrete problem consists of finding $u_h \in V_h$ such that

$$B_h(u_h, v_h) = (f, v_h)_{0,\Omega} \qquad \forall v_h \in V_h. \tag{10}$$

The penalty parameter γ is defined as

$$\forall F \in \mathscr{F}_h, \qquad \gamma = \alpha \frac{\gamma_K}{h_F} + \gamma_\beta, \tag{11}$$

where α is a positive scalar (α can also vary from face to face) and where

$$\forall F \in \mathscr{F}_h^i, \qquad \gamma_K = (\omega^-)^2 \delta_{Kn}^- + (\omega^+)^2 \delta_{Kn}^+ \tag{12}$$

$$\forall F \in \mathscr{F}_h^{\partial\Omega}, \qquad \gamma_K = \delta_{Kn}, \tag{13}$$

$$\forall F \in \mathscr{F}_h, \qquad \gamma_\beta = \tfrac{1}{2}|\beta \cdot n_F|, \tag{14}$$

with $\delta_{Kn}^{\mp} = n_F^t K^{\mp} n_F$ if $F \in \mathscr{F}_h^i$ and $\delta_{Kn} = n_F^t K n_F$ if $F \in \mathscr{F}_h^{\partial\Omega}$. Note that the choice for γ_β amounts to the usual upwind scheme to stabilize the advective derivative. As for any symmetric IP method, the size of the penalty parameter α is assumed to be large enough. This assumption is made for the rest of this work. The minimal value for α depends on the actual value of the constant arising in the trace inequality (17) stated below; it can be determined from the proof of Lemma 3.1 to ensure coercivity. Because they are standard, these developments are omitted.

For the error analysis in the energy norm (see Section 3), no other assumption than (6) is made for the weights. In particular, it is possible to choose $\omega^{\mp} = \frac{1}{2}$, in which case the SWIP bilinear form B_h reduces to the standard IP bilinear form with the penalty parameter scaling as the standard average of the diffusivity in the normal direction; this method has been analyzed in [11]. Note also that the choice made in [15] for the penalty parameter is different since it involves the maximum eigenvalue of K.

For the error analysis in the advective derivative (see Section 4), a specific choice of the weights differing from $\omega^{\mp} = \frac{1}{2}$ has to be made to yield robust error estimates with respect to the diffusivity. Specifically, we shall set

$$\omega^- = \frac{\delta_{Kn}^+}{\delta_{Kn}^+ + \delta_{Kn}^-}, \qquad \omega^+ = \frac{\delta_{Kn}^-}{\delta_{Kn}^+ + \delta_{Kn}^-}, \tag{15}$$

and thus

$$\forall F \in \mathscr{F}_h^i, \qquad \gamma_K = \frac{\delta_{Kn}^+ \delta_{Kn}^-}{\delta_{Kn}^+ + \delta_{Kn}^-}. \tag{16}$$

Note that with this choice $\gamma_K = \omega^- \delta_{Kn}^- = \omega^+ \delta_{Kn}^+$, and that $2\gamma_K$ is the harmonic average of the normal component of the diffusivity tensor across the interface. Observe also that $\gamma_K \leq \inf(\delta_{Kn}^-, \delta_{Kn}^+)$, a point that becomes important to ensure even the consistency of the method when the diffusivity is actually allowed to vanish locally, see [6]. The numerical results presented in Section 5 show that also in the energy norm, the DG method behaves better if the weights are chosen according to (15). Hence, we recommend this choice whenever the diffusivity exhibits heterogeneities.

3 Error analysis in the energy norm

The goal of this section is to establish an error estimate for the SWIP method in the energy norm, the estimate being robust with respect to heterogeneities and anisotropies in the diffusivity. The analysis is performed using fairly standard arguments, i.e., by establishing coercivity, consistency and continuity properties for the SWIP bilinear form in the spirit of Strang's Second Lemma [9].

In the sequel, the symbol $\lesssim$ indicates an inequality involving a positive constant C independent of the mesh family and of the diffusivity. The constant C can depend on $\|\beta\|_{[W^{1,\infty}(\Omega)]^d}$, $\|\mu\|_{L^{\infty}(\Omega)}$, μ_0^{-1} (see (3)), and the shape-regularity of the mesh family. Without loss of generality, it can be assumed that the problem data is normalized so that $\|\beta\|_{[W^{1,\infty}(\Omega)]^d}$ is of order unity. We will not be concerned with the dependency on $\|\mu\|_{L^{\infty}(\Omega)}$ since we are not interested in strong reaction regimes. The dependency on μ_0^{-1} can be addressed by means of Poincaré inequalities; this will not be further discussed here. Owing to the shape-regularity of the mesh family, the following inverse trace and inverse inequalities hold: For all $T \in \mathcal{T}_h$ and for all $v_h \in V_h$,

$$\|v_h\|_{0,\partial T} \lesssim h_T^{-\frac{1}{2}} \|v_h\|_{0,T}, \tag{17}$$

$$\|\nabla_h v_h\|_{0,T} \lesssim h_T^{-1} \|v_h\|_{0,T}, \tag{18}$$

which result from the shape regularity of the mesh family $\{\mathcal{T}_h\}_{h>0}$.

For a function $v \in V(h)$, we consider the following jump seminorms

$$|[\![v]\!]|_{\sigma}^2 = \sum_{F \in \mathcal{F}_h} |[\![v]\!]|_{\sigma,F}^2, \qquad |[\![v]\!]|_{\sigma,F}^2 = (\sigma[\![v]\!], [\![v]\!])_{0,F}, \tag{19}$$

with $\sigma := \gamma_\beta$, $\sigma := \gamma_K$ or $\sigma := \gamma$. The natural energy norm with which to equip $V(h)$ is

$$\|v\|_{h,B} = \|v\|_{0,\Omega} + \|\kappa\nabla_h v\|_{0,\Omega} + |[\![v]\!]|_{\gamma} \tag{20}$$

where κ denotes the (unique) symmetric positive definite tensor-valued field such that $\kappa^2 = K$ a.e. in Ω.

LEMMA 3.1 *(Coercivity)* The bilinear form B_h is $\|\cdot\|_{h,B}$-coercive, i.e., for all $v_h \in V_h$,

$$B_h(v_h, v_h) \gtrsim \|v_h\|_{h,B}^2. \tag{21}$$

Proof. Let $v_h \in V_h$. Taking $v = w = v_h$ in (8) yields

$$B_h(v_h, v_h) = \|\kappa\nabla_h v_h\|_{0,\Omega}^2 + (\mu v_h, v_h)_{0,\Omega} - ((\nabla \cdot \beta)v_h, v_h)_{0,\Omega} - (v_h, \beta \cdot \nabla_h v_h)_{0,\Omega}$$
$$+ |[\![v_h]\!]|_{\gamma}^2 - \sum_{F \in \mathcal{F}_h} 2(n_F^t \{K\nabla v_h\}_\omega, [\![v_h]\!])_{0,F}$$
$$+ \sum_{F \in \mathcal{F}_h^i} (\beta \cdot n_F \{v_h\}, [\![v_h]\!])_{0,F} + \sum_{F \in \mathcal{F}_h^{\partial\Omega}} \tfrac{1}{2}(\beta \cdot n_F v_h, v_h)_{0,F}. \tag{22}$$

6

Integrating by parts the fourth term on the right hand side of (22) and owing to hypothesis (3), we obtain

$$(\mu v_h, v_h)_{0,\Omega} - ((\nabla \cdot \beta) v_h, v_h)_{0,\Omega} - (v_h, \beta \cdot \nabla_h v_h)_{0,\Omega} \tag{23}$$
$$+ \sum_{F \in \mathscr{F}_h^i} (\beta \cdot n_F \{v_h\}, [\![v_h]\!])_{0,F} + \sum_{F \in \mathscr{F}_h^{\partial \Omega}} \tfrac{1}{2} (\beta \cdot n_F v_h, v_h)_{0,F} = ((\mu - \tfrac{1}{2} \nabla \cdot \beta) v_h, v_h)_{0,\Omega} \gtrsim \|v_h\|_{0,\Omega}^2.$$

Consider now the sixth term in the right-hand side of (22). Let $F \in \mathscr{F}_h$. First, observe that owing to Young's inequality

$$|2(n_F^t \omega^{\mp} (K \nabla_h v_h)^{\mp}, [\![v_h]\!])_{0,F}| = |2((\kappa \nabla_h v_h)^{\mp}, \omega^{\mp} \kappa^{\mp} n_F [\![v_h]\!])_{0,F}|$$
$$\leq h_F \alpha_0 \|(\kappa \nabla_h v_h)^{\mp}\|_{0,F}^2 + \frac{1}{\alpha_0} \left(\frac{(\omega^{\mp})^2 \delta_{Kn}^{\mp}}{h_F} [\![v_h]\!], [\![v_h]\!] \right)_{0,F},$$

where $\alpha_0 > 0$ can be chosen as small as needed. Using the trace inverse inequality (17) and the definition of γ_K (12)-(13) yields

$$|2(n_F^t \{K \nabla_h v_h\}_\omega, [\![v_h]\!])_{0,F}| \lesssim \alpha_0 \|\kappa \nabla_h v_h\|_{0,\mathscr{T}(F)}^2 + \frac{1}{\alpha_0 h_F} |[\![v_h]\!]|_{\gamma_K, F}^2.$$

The end of the proof is classical since α in (11) can be chosen to be large enough. $\quad \square$

LEMMA 3.2 *(Consistency)* Let u solve (2) and let u_h solve (10). Assume that $u \in H^2(\mathscr{T}_h)$. Then

$$\forall v_h \in V_h, \qquad B_h(u - u_h, v_h) = 0 \tag{24}$$

Proof. Let $v_h \in V_h$. Since $u \in H_0^1(\Omega)$, (9) yields

$$B_h(u, v_h) = (K \nabla u, \nabla_h v_h)_{0,\Omega} + (\mu u, v_h)_{0,\Omega} + (\beta \cdot \nabla u, v_h)_{0,\Omega} - \sum_{F \in \mathscr{F}_h} (n_F^t \{K \nabla u\}_\omega, [\![v_h]\!])_{0,F}.$$

Using the fact that $n_F^t K \nabla u$ is continuous on interior faces yields $n_F^t \{K \nabla u\}_\omega = (\omega^- + \omega^+) n_F^t K \nabla u = n_F^t K \nabla u$ owing to (6). Hence, integrating by parts leads to

$$(K \nabla u, \nabla_h v_h)_{0,\Omega} - \sum_{F \in \mathscr{F}_h} (n_F^t \{K \nabla u\}_\omega, [\![v_h]\!])_{0,F} = - \sum_{T \in \mathscr{T}_h} (\nabla \cdot (K \nabla u), v_h)_{0,T}.$$

As a result,

$$B_h(u, v_h) = \sum_{T \in \mathscr{T}_h} (-\nabla \cdot (K \nabla u) + \beta \cdot \nabla u + \mu u, v_h)_{0,T} = (f, v_h)_{0,\Omega} = B_h(u_h, v_h),$$

yielding (24). $\quad \square$

We now establish a continuity property for the SWIP bilinear form B_h. To this purpose, we introduce on $V(h)$ the norm

$$\|v\|_{h, \frac{1}{2}} = \|v\|_{h,B} + \left(\sum_{T \in \mathscr{T}_h} \|v\|_{0, \partial T}^2 \right)^{\frac{1}{2}} + \left(\sum_{T \in \mathscr{T}_h} h_T \|\kappa \nabla_h v\|_{0, \partial T}^2 \right)^{\frac{1}{2}}. \tag{25}$$

Let $V_h^\perp = \{v \in V(h), \forall v_h \in V_h, (v, v_h)_{0,\Omega} = 0\}$.

LEMMA 3.3 *(Continuity)* The following holds:

$$\forall (v, w_h) \in V_h^\perp \times V_h, \qquad |B_h(v, w_h)| \lesssim \|v\|_{h,\frac{1}{2}} \|w_h\|_{h,B}. \tag{26}$$

Proof. Let $(v, w_h) \in V_h^\perp \times V_h$. The first two terms in (8) are easily bounded as

$$|(K\nabla_h v, \nabla_h w_h)_{0,\Omega}| + |((\mu - \nabla\cdot\beta)v, w_h)_{0,\Omega}| \lesssim \|v\|_{h,B} \|w_h\|_{h,B}.$$

To bound the third term, let $\overline{\beta}$ be the piecewise constant, vector-valued field equal to the mean value of β on each $T \in \mathcal{T}_h$. Then,

$$(v, \beta\cdot\nabla_h w_h)_{0,\Omega} = (v, \overline{\beta}\cdot\nabla_h w_h)_{0,\Omega} + (v, (\beta - \overline{\beta})\cdot\nabla_h w_h)_{0,\Omega}$$
$$= (v, (\beta - \overline{\beta})\cdot\nabla_h w_h)_{0,\Omega},$$

since $\overline{\beta}\cdot\nabla_h w_h \in V_h$ and $v \in V_h^\perp$. Moreover, since $\beta \in [W^{1,\infty}(\Omega)]^d$,

$$\forall T \in \mathcal{T}_h, \qquad \|\beta - \overline{\beta}\|_{[L^\infty(T)]^d} \lesssim h_T,$$

so that the inverse inequality (18) yields

$$|(v, \beta\cdot\nabla_h w_h)_{0,\Omega}| \lesssim \|v\|_{0,\Omega} \|w_h\|_{0,\Omega} \leq \|v\|_{h,B} \|w_h\|_{h,B}.$$

Furthermore, proceeding as in the proof of Lemma 3.1 yields, for all $F \in \mathcal{F}_h$,

$$|(n_F^t \{K\nabla_h v\}_\omega, [\![w_h]\!])_{0,F}| \lesssim \left(\sum_{T \in \mathcal{T}(F)} h_T^{\frac{1}{2}} \|\kappa\nabla_h v\|_{0,\partial T} \right) h_F^{-\frac{1}{2}} |[\![w_h]\!]|_{\gamma_K, F}$$

and

$$|(n_F^t \{K\nabla_h w_h\}_\omega, [\![v]\!])_{0,F}| \lesssim h_F^{-\frac{1}{2}} |[\![v]\!]|_{\gamma_K, F} \|\kappa\nabla_h w_h\|_{0,\mathcal{T}(F)},$$

so that

$$\sum_{F \in \mathcal{F}_h} \left(|(n_F^t \{K\nabla v\}_\omega, [\![w_h]\!])_{0,F}| + |(n_F^t \{K\nabla w_h\}_\omega, [\![v]\!])_{0,F}| \right) \lesssim \|v\|_{h,\frac{1}{2}} \|w_h\|_{h,B}.$$

For the remaining terms, we obtain

$$\sum_{F \in \mathcal{F}_h} |(\gamma[\![v]\!], [\![w_h]\!])_{0,F}| + \sum_{F \in \mathcal{F}_h^i} |(\beta\cdot n_F \{v\}, [\![w_h]\!])_{0,F}| + \sum_{F \in \mathcal{F}_h^{\partial\Omega}} |\tfrac{1}{2}(\beta\cdot n_F v, w_h)_{0,F}|$$

$$\lesssim |[\![v]\!]|_\gamma |[\![w_h]\!]|_\gamma + \sum_{F \in \mathcal{F}_h^i} \|\{v\}\|_{0,F} |[\![w_h]\!]|_{\gamma_\beta, F} \leq \|v\|_{h,\frac{1}{2}} \|w_h\|_{h,B}.$$

This completes the proof since $\|\cdot\|_{h,B} \leq \|\cdot\|_{h,\frac{1}{2}}$. $\qquad\qquad\square$

THEOREM 3.1 Let $\Pi_h u$ be the L^2-projection of u onto V_h. Then,

$$\|u - u_h\|_{h,B} \lesssim \|u - \Pi_h u\|_{h,\frac{1}{2}}. \tag{27}$$

8

Proof. Owing to Lemmata 3.1, 3.2 and 3.3,

$$\|u_h - \Pi_h u\|_{h,B} \lesssim \frac{B_h(u_h - \Pi_h u, u_h - \Pi_h u)}{\|u_h - \Pi_h u\|_{h,B}} = \frac{B_h(u - \Pi_h u, u_h - \Pi_h u)}{\|u_h - \Pi_h u\|_{h,B}}$$
$$\lesssim \|u - \Pi_h u\|_{h,\frac{1}{2}}. \tag{28}$$

We complete the proof by applying the triangle inequality and using the fact that $\|\cdot\|_{h,B} \leq \|\cdot\|_{h,\frac{1}{2}}$. $\qquad\square$

REMARK 3.1 Estimate (27) yields an error upper bound in the natural energy norm with a constant independent of the diffusivity tensor. Furthermore, if the exact solution is smooth enough locally on each mesh cell, namely $u \in H^{p+1}(\mathcal{T}_h)$, it is readily seen using standard approximation properties for the L^2-orthogonal projector Π_h, that the upper bound converges as h^p, which is optimal.

We now prove that under some assumptions, the error estimate in the L^2-norm can be improved using the Aubin-Nitsche duality argument. Let $\lambda_{m,K}$ denote the lowest eigenvalue of K in Ω and set $\lambda_{M,K} = \max(1, \lambda_K)$ where λ_K denotes the largest eigenvalue of K in Ω. We introduce the following dual problem: seek $\psi \in H_0^1(\Omega)$ such that

$$(K\nabla v, \nabla \psi)_{0,\Omega} + (\beta \cdot \nabla v, \psi)_{0,\Omega} + (\mu v, \psi)_{0,\Omega} = (v, u - u_h)_{0,\Omega} \quad \forall v \in H_0^1(\Omega). \tag{29}$$

We assume that elliptic regularity holds in the broken H^2-norm, namely that

$$\|\psi\|_{H^2(\mathcal{T}_h)} \lesssim \lambda_{m,K}^{-1} \|u - u_h\|_{0,\Omega}. \tag{30}$$

When K is uniform, it is well-known that the convexity of Ω is sufficient to guarantee (30). This is no longer the case if K is discontinuous. In this case, (30) implicitly amounts to additional assumptions on the distribution of K inside Ω.

THEOREM 3.2 In the above framework,

$$\|u - u_h\|_{0,\Omega} \leq \frac{\lambda_{M,K}^{\frac{1}{2}}}{\lambda_{m,K}} h \left(\|u - u_h\|_{h,B} + \inf_{w_h \in V_h} \|u - w_h\|_{h,B_+} \right) \tag{31}$$

where for all $v \in V(h)$,

$$\|v\|_{h,B_+} = \|v\|_{h,B} + \left(\sum_{T \in \mathcal{T}_h} h_T^2 \|\nabla_h v\|_{0,T}^2 \right)^{\frac{1}{2}} + \left(\sum_{T \in \mathcal{T}_h} h_T \|\kappa \nabla_h v\|_{0,\partial T}^2 \right)^{\frac{1}{2}}. \tag{32}$$

Proof. Step (i): observe that for all $v \in V(h)$, using (8) yields

$$B_h(v, \psi) = (K\nabla_h v, \nabla \psi)_{0,\Omega} + ((\mu - \nabla \cdot \beta) v, \psi)_{0,\Omega} - (v, \beta \cdot \nabla \psi)_{0,\Omega} - \sum_{F \in \mathcal{F}_h} (n_F^t \{K\nabla \psi\}_\omega, [\![v]\!])_{0,F}$$
$$= \sum_{T \in \mathcal{T}_h} (v, -\nabla \cdot (K\nabla \psi) - \beta \cdot \nabla \psi + (\mu - \nabla \cdot \beta) \psi)_{0,T} = (v, u - u_h)_{0,\Omega}. \tag{33}$$

Step (ii): define on $V(h)$ the norm

$$\|v\|_{h,1} = \|v\|_{h,\frac{1}{2}} + \left(\sum_{T \in \mathcal{T}_h} h_T^{-2} \|v\|_{0,T}^2 \right)^{\frac{1}{2}}, \tag{34}$$

9

and let us prove that for all $(v, w) \in V(h) \times V(h)$,

$$|B_h(v, w)| \lesssim \|v\|_{h, B_+} \|w\|_{h, 1}. \tag{35}$$

Indeed, indicating by T_i, $1 \leq i \leq 8$, the eight terms on the right-hand side of (9), and proceeding as in the proof of Lemma 3.3, it is clear that $\sum_{i \neq 3} |T_i| \lesssim \|v\|_{h, B_+} \|w\|_{h, \frac{1}{2}}$.
Moreover,

$$|T_3| = |(\beta \cdot \nabla_h v, w)_{0, \Omega}| \lesssim \sum_{T \in \mathscr{T}_h} \|\nabla_h v\|_{0, T} \|w\|_{0, T} = \sum_{T \in \mathscr{T}_h} h_T \|\nabla_h v\|_{0, T} h_T^{-1} \|w\|_{0, T} \leq \|v\|_{h, B_+} \|w\|_{h, 1}.$$

Hence, (35) holds.
Step (iii): taking $v = u - u_h$ in (33), applying Lemma 3.2 and using (35) yields for all $\psi_h \in V_h$,

$$\|u - u_h\|_{0, \Omega}^2 = B_h(u - u_h, \psi) = B_h(u - u_h, \psi - \psi_h) \lesssim \|u - u_h\|_{h, B_+} \|\psi - \psi_h\|_{h, 1}.$$

Using standard interpolation results leads to

$$\inf_{\psi_h \in V_h} \|\psi - \psi_h\|_{h, 1} \lesssim \lambda_{M, K}^{\frac{1}{2}} h \|\psi\|_{H^2(\mathscr{T}_h)},$$

and taking into account (30) yields

$$\|u - u_h\|_{0, \Omega} \lesssim \frac{\lambda_{M, K}^{\frac{1}{2}}}{\lambda_{m, K}} h \|u - u_h\|_{h, B_+}. \tag{36}$$

Using the inverse inequalities (17) and (18), we infer that for all $v_h \in V_h$,

$$\|v_h\|_{h, B_+} \lesssim \|v_h\|_{h, B} + \|v_h\|_{0, \Omega} + \|\kappa \nabla_h v_h\|_{0, \Omega} \lesssim \|v_h\|_{h, B}. \tag{37}$$

Applying the triangle inequality together with (37) leads to

$$\begin{aligned}
\|u - u_h\|_{h, B_+} &\leq \|u - w_h\|_{h, B_+} + \|u_h - w_h\|_{h, B_+} \\
&\lesssim \|u - w_h\|_{h, B_+} + \|u_h - w_h\|_{h, B} \\
&\lesssim \|u - w_h\|_{h, B_+} + \|u - u_h\|_{h, B},
\end{aligned} \tag{38}$$

where w_h is arbitrary in V_h. Substituting (38) into (36) yields (31). $\qquad \square$

COROLLARY 3.1 If the exact solution u is in $H^{p+1}(\mathscr{T}_h)$, then

$$\|u - u_h\|_{0, \Omega} \lesssim \frac{\lambda_{M, K}}{\lambda_{m, K}} h^{p+1} \|u\|_{H^{p+1}(\mathscr{T}_h)}. \tag{39}$$

Proof. Use Theorem 3.2 and standard approximation properties of V_h. $\qquad \square$

4 Error analysis for the advective derivative

When the diffusivity takes small values, it is no longer possible to control the advective derivative by means of Theorem 3.1. The goal of this section is to obtain a control of

10

the error in the advective derivative that is possibly robust with respect to the diffusivity. Define on $V(h)$ the norm

$$\|v\|_{h,B\beta} = \|v\|_{h,B} + \|v\|_{h,\beta}, \tag{40}$$

where

$$\|v\|_{h,\beta} = \left(\sum_{T \in \mathscr{T}_h} h_T \|\beta \cdot \nabla_h v\|_{0,T}^2 \right)^{\frac{1}{2}}. \tag{41}$$

To prove a convergence result in the $\|\cdot\|_{h,B\beta}$-norm, the first step is to derive a stability property for the SWIP bilinear form B_h in this norm.

LEMMA 4.1 *(Stability)* Define

$$\forall T \in \mathscr{T}_h, \qquad \Delta_{K,T} = \begin{cases} 1 & \text{if } \|\beta\|_{[L^\infty(T)]^d} \gtrsim \frac{\lambda_{M,T}}{h_T}, \\ \frac{\lambda_{M,T}}{\lambda_{m,T}} & \text{otherwise}, \end{cases} \tag{42}$$

where $\lambda_{M,T}$ and $\lambda_{m,T}$ are respectively the maximum and the minimum eigenvalue of $K|_T$. Set $\Delta_K = \max_{T \in \mathscr{T}_h} \Delta_{K,T}$. Then,

$$\inf_{v_h \in V_h \setminus \{0\}} \sup_{w_h \in V_h \setminus \{0\}} \frac{B_h(v_h, w_h)}{\|v_h\|_{h,B\beta} \|w_h\|_{h,B\beta}} \gtrsim \Delta_K^{-1}. \tag{43}$$

REMARK 4.1 We stress the fact that the inf-sup condition is robust in the isotropic case and in the anisotropic case if the cell Péclet numbers evaluated with the largest eigenvalue of the diffusivity tensor are large enough. Note also that the anisotropies are local to the mesh element, i.e., ratios of eigenvalues between adjacent elements are not considered. To achieve this result, the key point (see the control of $|[\![\pi_h]\!]|^2_{\gamma_K}$ in the proof below) is that the choice (15) for the weights yields $\gamma_K \leq \inf(\delta_{Kn}^-, \delta_{Kn}^+)$.

Proof. Let $v_h \in V_h$ and set $\mathbf{S} = \sup_{w_h \in V_h \setminus \{0\}} \frac{B_h(v_h, w_h)}{\|w_h\|_{h,B\beta}}$. We want to prove that $\|v_h\|_{h,B\beta} \lesssim \Delta_K \mathbf{S}$.

Step (i): owing to Lemma 3.1, we infer that

$$\|v_h\|_{h,B}^2 \lesssim \mathbf{S} \|v_h\|_{h,B\beta}, \tag{44}$$

so it only remains to control the advective derivative in $\|v_h\|_{h,B\beta}$.

Step (ii): let $\pi_h \in V_h$ be such that for all $T \in \mathscr{T}_h$ $\pi_h|_T = h_T \overline{\beta} \cdot \nabla_h v_h$ where $\overline{\beta}$ is defined in the proof of Lemma 3.3. Let us prove that

$$\|\pi_h\|_{h,B\beta} \lesssim \Delta_K^{\frac{1}{2}} \|v_h\|_{h,B\beta}. \tag{45}$$

The inverse inequality (18) and the regularity of β yield for all $T \in \mathscr{T}_h$,

$$\|\pi_h\|_{0,T} \lesssim h_T \|\beta \cdot \nabla_h v_h\|_{0,T} + h_T \|v_h\|_{0,T}, \tag{46}$$

while the inverse inequality (17) yields for all $F \in \mathscr{F}_h$

$$|[\![\pi_h]\!]|^2_{\gamma_\beta,F} \lesssim \sum_{T \in \mathscr{T}(F)} \|\pi_h\|_{0,\partial T}^2 \lesssim \sum_{T \in \mathscr{T}(F)} \left(h_T \|\beta \cdot \nabla_h v_h\|_{0,T}^2 + h_T \|v_h\|_{0,T}^2 \right).$$

11

Hence, since $\Delta_K \geq 1$,

$$\|\pi_h\|_{0,\Omega} + |[\![\pi_h]\!]|_{\gamma_\beta} \lesssim \|v_h\|_{h,B\beta} \leq \Delta_K^{\frac{1}{2}}\|v_h\|_{h,B\beta}.$$

Let us estimate $h_F^{-\frac{1}{2}}|[\![\pi_h]\!]|_{\gamma_K,F}$ for all $F \in \mathscr{F}_h$. Observe first that $\gamma_K = \omega^\mp \delta_{Kn}^\mp \leq \delta_{Kn}^\mp$ if $F \in \mathscr{F}_h^i$ and $\gamma_K = \delta_{Kn}$ if $F \in \mathscr{F}_h^{\partial\Omega}$. Hence, if there is a $T \in \mathscr{T}_h(F)$ such that $\|\beta\|_{[L^\infty(T)]^d} \gtrsim \frac{\lambda_{M,T}}{h_T}$, then

$$h_F^{-1}|[\![\pi_h]\!]|_{\gamma_K,F}^2 \leq h_F^{-1}\lambda_{M,T}\|[\![\pi_h]\!]\|_{0,F}^2 \leq \sum_{T \in \mathscr{T}(F)} \left(h_T\|\beta\cdot\nabla_h v_h\|_{0,T}^2 + h_T\|v_h\|_{0,T}^2\right).$$

Otherwise, for all $F \in \mathscr{F}_h^i$,

$$h_F^{-1}\gamma_K[\![\pi_h]\!]^2 \lesssim h_F\gamma_K\left(((\overline{\beta}\cdot\nabla_h v_h)^-)^2 + ((\overline{\beta}\cdot\nabla_h v_h)^+)^2\right)$$
$$\lesssim h_F\left(\delta_{K,n}^-((\overline{\beta}\cdot\nabla_h v_h)^-)^2 + \delta_{K,n}^+((\overline{\beta}\cdot\nabla_h v_h)^+)^2\right),$$

and similarly for $F \in \mathscr{F}_h^{\partial\Omega}$. Hence, using the trace inverse inequality (17),

$$h_F^{-1}|[\![\pi_h]\!]|_{\gamma_K,F}^2 \lesssim \sum_{T \in \mathscr{T}(F)} \lambda_{M,T}\|\nabla_h v_h\|_{0,T}^2 \lesssim \sum_{T \in \mathscr{T}(F)} \frac{\lambda_{M,T}}{\lambda_{m,T}}\|\kappa\nabla_h v_h\|_{0,T}^2.$$

Thus, $|[\![\pi_h]\!]|_\gamma \lesssim \Delta_K^{\frac{1}{2}}\|v_h\|_{h,B\beta}$. Furthermore, since κ is piecewise constant,

$$\|\kappa\nabla_h\pi_h\|_{0,T} = h_T\|\overline{\beta}\cdot\nabla_h(\kappa\nabla_h v_h)\|_{0,T} \lesssim \|\kappa\nabla_h v_h\|_{0,T},$$

implying that $\|\kappa\nabla_h\pi_h\|_{0,\Omega} \lesssim \|v_h\|_{h,B}$. Finally, the advective derivative of π_h is controlled by

$$\|\pi_h\|_{h,\beta}^2 \lesssim \sum_{T \in \mathscr{T}_h} h_T^{-1}\|\pi_h\|_{0,T}^2 \lesssim \|v_h\|_{h,B\beta}^2,$$

owing to (46). This proves (45).
Step (iii): we can now examine the term $\|v_h\|_{h,\beta}^2$ by making use of (9):

$$\|v_h\|_{h,\beta}^2 = B_h(v_h,\pi_h) - (K\nabla_h v_h,\nabla_h\pi_h)_{0,\Omega} - (\mu v_h,\pi_h)_{0,\Omega}$$
$$+ \sum_{T \in \mathscr{T}_h}(\beta\cdot\nabla_h v_h, h_T\beta\cdot\nabla_h v_h - \pi_h)_{0,T} + \sum_{F \in \mathscr{F}_h^i}(\beta\cdot n_F\{\pi_h\}, [\![v_h]\!])_{0,F}$$
$$+ \sum_{F \in \mathscr{F}_h^{\partial\Omega}}\tfrac{1}{2}(\beta\cdot n_F v_h, \pi_h)_{0,F} - \sum_{F \in \mathscr{F}_h}(\gamma[\![v_h]\!], [\![\pi_h]\!])_{0,F}$$
$$+ \sum_{F \in \mathscr{F}_h}\left((n_F^t\{K\nabla_h v_h\}_\omega, [\![\pi_h]\!])_{0,F} + (n_F^t\{K\nabla_h\pi_h\}_\omega, [\![v_h]\!])_{0,F}\right)$$
$$= B_h(v_h,\pi_h) + T_1 + T_2 + T_3 + T_4 + T_5 + T_6 + T_7 + T_8.$$

We observe that

$$|B_h(v_h,\pi_h)| \leq \mathbf{S}\|\pi_h\|_{h,B\beta} \leq \mathbf{S}\Delta_K^{\frac{1}{2}}\|v_h\|_{h,B\beta}.$$

12

It is also clear that

$$|T_1| + |T_2| + |T_6| + |T_7| + |T_8| \lesssim \|v_h\|_{h,B} \|\pi_h\|_{h,B} \lesssim \mathbf{S}^{\frac{1}{2}} \Delta_K^{\frac{1}{2}} \|v_h\|_{h,B\beta}^{\frac{3}{2}}.$$

Furthermore, using the inverse inequality (17) together with (46) yields

$$|T_4| + |T_5| \lesssim |[[v_h]]|_{\gamma_\beta} \left(\sum_{T \in \mathscr{T}_h} \|\pi_h\|_{0,\partial T}^2 \right)^{\frac{1}{2}} \lesssim |[[v_h]]|_{\gamma_\beta} \left(\sum_{T \in \mathscr{T}_h} h_T^{-1} \|\pi_h\|_{0,T}^2 \right)^{\frac{1}{2}}$$

$$\lesssim \|v_h\|_{h,B} \|v_h\|_{h,B\beta} \lesssim \mathbf{S}^{\frac{1}{2}} \|v_h\|_{h,B\beta}^{\frac{3}{2}}.$$

Finally,

$$|T_3| \leq \sum_{T \in \mathscr{T}_h} h_T |(\beta \cdot \nabla_h v_h, (\beta - \overline{\beta}) \cdot \nabla_h v_h)_{0,T}| \lesssim \sum_{T \in \mathscr{T}_h} h_T^2 \|\beta \cdot \nabla_h v_h\|_{0,T} \|\nabla_h v_h\|_{0,T}$$

$$\lesssim \sum_{T \in \mathscr{T}_h} h_T \|\beta \cdot \nabla_h v_h\|_{0,T} \|v_h\|_{0,T} \lesssim \|v_h\|_{h,B\beta} \|v_h\|_{0,\Omega} \lesssim \mathbf{S}^{\frac{1}{2}} \|v_h\|_{h,B\beta}^{\frac{3}{2}}.$$

Hence,

$$\|v_h\|_{h,B\beta}^2 \lesssim \|v_h\|_{h,B}^2 + \|v_h\|_{h,\beta}^2$$

$$\lesssim \mathbf{S}\|v_h\|_{h,B\beta} + \mathbf{S}\Delta_K^{\frac{1}{2}} \|v_h\|_{h,B\beta} + \mathbf{S}^{\frac{1}{2}}\Delta_K^{\frac{1}{2}} \|v_h\|_{h,B\beta}^{\frac{3}{2}} + \mathbf{S}^{\frac{1}{2}} \|v_h\|_{h,B\beta}^{\frac{3}{2}}$$

$$\lesssim \mathbf{S}\Delta_K^{\frac{1}{2}} \|v_h\|_{h,B\beta} + \mathbf{S}^{\frac{1}{2}}\Delta_K^{\frac{1}{2}} \|v_h\|_{h,B\beta}^{\frac{3}{2}},$$

where we have used the fact that $\Delta_K \geq 1$ in the last step. Applying twice Young's inequality yields the desired result. $\square$

Proceeding as above, the following result is readily inferred:

THEOREM 4.1 In the above framework,

$$\|u - u_h\|_{h,B\beta} \lesssim \Delta_K \inf_{v_h \in V_h} \|u - v_h\|_{h,\frac{1}{2}\beta}, \tag{47}$$

where, for all $v \in V(h)$,

$$\|v\|_{h,\frac{1}{2}\beta} = \|v\|_{h,B\beta} + \left(\sum_{T \in \mathscr{T}_h} \|v\|_{0,\partial T}^2 \right)^{\frac{1}{2}} + \left(\sum_{T \in \mathscr{T}_h} h_T \|\kappa \nabla_h v\|_{0,\partial T}^2 \right)^{\frac{1}{2}}. \tag{48}$$

REMARK 4.2 Estimate (47) yields an error upper bound on the advective derivative with a constant depending on Δ_K. Robustness is recovered whenever $\Delta_K = 1$, i.e., when working with an isotropic diffusivity tensor or when the cell Péclet numbers evaluated with the largest eigenvalue of the diffusivity tensor are large enough. Furthermore, if $u \in H^{p+1}(\mathscr{T}_h)$, the upper bound converges as $h^{p+\frac{1}{2}}$, which is optimal.

5 Numerical tests

5.1 A test case with discontinuous coefficients

To verify the convergence of the SWIP method and to make quantitative comparisons between this and other IP methods, we consider the test problem proposed in [3],

featuring discontinuous coefficients and where the exact solution is known analytically. We split the domain $\Omega = [0,1] \times [0,1]$ into two subdomains: $\Omega_1 = [0, \frac{1}{2}] \times [0,1]$, $\Omega_2 = [\frac{1}{2}, 1] \times [0,1]$. The diffusivity tensor K is constant within each subdomain, and defined as

$$K(x,y) = \begin{pmatrix} \varepsilon(x) & 0 \\ 0 & 1.0 \end{pmatrix}$$

where $\varepsilon(x)$ is a discontinuous function across the interface $x = \frac{1}{2}$. Indicating with the subscript 1 (resp. 2) the restriction to the subdomain Ω_1 (resp. Ω_2), we will consider different values of ε_1, while ε_2 is set equal to 1. Letting $\beta = (1,0)^t$, $\mu = 0$ and $f = 0$, the exact solution is independent of the y-coordinate, and is exponential with respect to the x-coordinate. The following conditions must be satisfied at the interface between the two subdomains:

$$\lim_{x \to \frac{1}{2}^-} u(x,y) = \lim_{x \to \frac{1}{2}^+} u(x,y), \text{ and } \lim_{x \to \frac{1}{2}^-} -\varepsilon_1 \partial_x u(x,y) = \lim_{x \to \frac{1}{2}^+} -\partial_x u(x,y).$$

Setting $u(0,y) = 1$, $u(1,y) = 0$ and applying the matching conditions, we obtain the value of the exact solution at the interface:

$$u\left(\frac{1}{2}, y\right) = \frac{\exp(\frac{1}{2\varepsilon_1})}{1 - \exp(\frac{1}{2\varepsilon_1})} \left(\frac{\exp(\frac{1}{2\varepsilon_1})}{1 - \exp(\frac{1}{2\varepsilon_1})} + \frac{1}{1 - \exp(\frac{1}{2})} \right)^{-1}.$$

As a result, the exact solution in each subdomain can be expressed as

$$u_1(x,y) = \frac{u(\frac{1}{2},y) - \exp(\frac{1}{2\varepsilon_1}) + (1 - u(\frac{1}{2},y))\exp(\frac{x}{\varepsilon_1})}{1 - \exp(\frac{1}{2\varepsilon_1})},$$

$$u_2(x,y) = \frac{-\exp(\frac{1}{2})u(\frac{1}{2},y) + u(\frac{1}{2},y)\exp(x - \frac{1}{2})}{1 - \exp(\frac{1}{2})}.$$

Table 1: Convergence rates of the SWIP method, $p = 1$

h	$\|u - u_h\|_{h,B}$	$\|u - u_h\|_{h,\beta}$	$\|u - u_h\|_{0,\Omega}$
0.1000	1.62e-01	1.49e-01	6.94e-03
0.0500	7.96e-02	5.45e-02	2.11e-03
0.0250	3.67e-02	1.87e-02	4.80e-04
0.0125	1.70e-02	6.37e-03	1.21e-04
order	1.11	1.55	1.98

To assess the accuracy of the SWIP method with respect to the mesh-size, we consider a family of uniform triangulations $\{\mathcal{T}_h\}_{h>0}$ which are conforming with respect to the interface between Ω_1 and Ω_2. These triangulations are obtained starting from a uniform partition of $\partial\Omega$ in sub-intervals of length $h = 0.1$, $h = 0.05$, $h = 0.025$ and $h = 0.0125$ respectively. The value of the penalty parameter α is henceforth set to $\alpha = 1.0$ for $\mathbb{P}_1$ elements and $\alpha = 4.0$ for $\mathbb{P}_2$ elements. The numerical results obtained with $\varepsilon_1 = 0.1$ are reported in Tables 1 and 2, where the order of convergence is computed with respect to the last two rows of each table. We observe that the SWIP method exhibits the orders of convergence predicted by the theory.

Table 2: Convergence rates of the SWIP method, $p = 2$

h	$\|u - u_h\|_{h,B}$	$\|u - u_h\|_{h,\beta}$	$\|u - u_h\|_{0,\Omega}$
0.1000	2.31e-02	2.15e-02	6.80e-04
0.0500	4.63e-03	3.31e-03	4.29e-05
0.0250	1.17e-03	5.93e-04	5.20e-06
0.0125	2.95e-04	1.05e-04	6.41e-07
order	1.99	2.49	3.02

Table 3: Comparison of SWIP and IP methods: $\varepsilon_1 = 5\text{e-}2$, $p = 1$

method	$\|u - u_h\|_{h,B}$	$\|u - u_h\|_{h,\beta}$	$\|u - u_h\|_{0,\Omega}$	M
SWIP	1.583e-01	1.505e-01	4.586e-03	9.555e-04
IP-A	1.483e-01	1.403e-01	5.153e-03	5.882e-03
IP-B	1.338e-01	1.378e-01	5.903e-03	5.882e-03

We have also compared the performance of the SWIP method with respect to two IP methods. The first method (IP-A) corresponds to the SWIP method with weights $\omega^{\mp} = \frac{1}{2}$. The penalty parameter γ_K is thus the arithmetic average of the diffusivity in the direction normal to the face. This method was analyzed in [11]. The second method (IP-B), proposed in [15], differs from IP-A in the choice of the penalty parameter: γ_K is the arithmetic average of the maximum eigenvalue of K on the triangles sharing the face F. We consider a uniform triangulation $\mathcal{T}_h$ characterized by $h = 0.05$. The quantitative analysis is based on the norms $\|\cdot\|_{h,B}$, $\|\cdot\|_{h,\beta}$, $\|\cdot\|_{0,\Omega}$ and the indicator

$$M = \max(|\max_{\Omega}(u_h) - \max_{\Omega}(u)|, |\min_{\Omega}(u_h) - \min_{\Omega}(u)|) \qquad (49)$$

which quantifies overshoots and undershoots of the calculated solution. The numerical results for $p = 1$ are found in Tables 3, 4, and in Figure 1. Table 3 deals with the case $\varepsilon_1 = 5\text{e-}2$; the inner layer is not very sharp and is resolved by the meshes under consideration. We observe that the three methods deliver similar results for all the quantities of interest. As the inner layer becomes sharper ($\varepsilon_1 = 5\text{e-}3$, Table 4), the SWIP scheme performs better than the other IP methods, especially in the L^2-norm and in the indicator M. The reason is that the weights permit sharper discontinuities in the calculated solution, leading to smaller oscillations in the internal layer, whereas the other IP methods force the discrete solution to be almost continuous. As can be observed in Figure 1, this limitation promotes instabilities in the neighborhood of the

Table 4: Comparison of SWIP and IP methods: $\varepsilon_1 = 5\text{e-}3$, $p = 1$

method	$\|u - u_h\|_{h,B}$	$\|u - u_h\|_{h,\beta}$	$\|u - u_h\|_{0,\Omega}$	M
SWIP	4.917e-01	1.280	1.474e-02	6.594e-02
IP-A	5.886e-01	1.303	4.973e-02	4.373e-01
IP-B	6.625e-01	1.634	7.553e-02	4.173e-01

Table 5: Comparison of SWIP and IP methods: $\varepsilon_1 = 5\text{e-}3$, $p = 2$

method	$\|u - u_h\|_{h,B}$	$\|u - u_h\|_{h,\beta}$	$\|u - u_h\|_{0,\Omega}$	M
SWIP	4.33e-01	1.44e+00	1.69e-02	6.72e-02
IP-A	6.05e-01	1.54e+00	3.77e-02	1.85e-01
IP-B	6.52e-01	1.71e+00	4.52e-02	1.86e-01

internal layer. The spurious oscillations generated in the case $\varepsilon_1 = 5\text{e-}3$ lead to an over-shoot of about 40%. The robustness of the SWIP method with respect to standard IP schemes is also confirmed by further numerical tests concerning vanishing values of ε_1 (Figure 2). Finally, Table 5 presents the results for $\varepsilon_1 = 5\text{e-}3$ and $p = 2$. We have in this case considered a coarser mesh yielding approximately the same number of degrees of freedom as in the simulations with linear polynomials. Then, the same conclusion as for $p = 1$ can be reached. As the mesh is further refined (or the polynomial degree is further increased), the approximation space eventually becomes rich enough to completely capture the internal layer, and the three methods (SWIP, IP-A and IP-B) exhibit a similar behavior.

5.2   A test case with genuine anisotropic properties

To conclude the sequence of numerical tests, we consider a test case with genuine anisotropic properties. Because of the complexity of the problem, it is not possible to compute analytically the exact solution. Consequently, the comparison between the SWIP and the IP methods will only be qualitative.

We consider the unit square $\Omega = [0,1] \times [0,1]$ split into four subdomains: $\Omega_1 = [0,\frac{2}{3}] \times [0,\frac{2}{3}]$, $\Omega_2 = [\frac{2}{3},1] \times [0,\frac{2}{3}]$, $\Omega_3 = [\frac{2}{3},1] \times [\frac{2}{3},1]$ and $\Omega_4 = [0,\frac{2}{3}] \times [\frac{2}{3},1]$. The diffusivity tensor K takes different values in each subregion:

$$K(x,y) = \begin{pmatrix} 1\text{e-}6 & 0 \\ 0 & 1.0 \end{pmatrix} \text{ for } (x,y) \in \Omega_1, \ \Omega_3,$$

$$K(x,y) = \begin{pmatrix} 1.0 & 0 \\ 0 & 1\text{e-}6 \end{pmatrix} \text{ for } (x,y) \in \Omega_2, \ \Omega_4.$$

For the advection term we consider a solenoidal field $\beta = (\beta_x, \beta_y)^t$ with $\beta_x = 40x(2y - 1)(x-1)$ and $\beta_y = -40y(2x-1)(y-1)$. Unlike the previous test case, we note that the field is neither constant nor orthogonal to the interfaces of discontinuity of K, but it is still oriented along the direction of increasing diffusivity, thus triggering internal layers. The forcing term only depends on the radial coordinate originating at the center of Ω in the form $f(x,y) = 10^{-2} \exp(-(r - 0.35)^2/0.005)$ with $r^2 = (x - 0.5)^2 + (y - 0.5)^2$; this corresponds to a Gaussian hill with center at $r = 0.35$. Finally, we choose $\mu = 1$. For the simulations, we consider a quasi-uniform mesh with $h = 0.025$. The mesh is conforming with respect to the discontinuities of K. A qualitative representation of the data is found in Figure 3.

In the left column of Figure 4 we compare the solutions obtained with the SWIP and the IP methods. The contour plots of the numerical solutions confirm that the methods at hand behave differently in the neighborhood of the interfaces where the tensor K is discontinuous. We observe that the SWIP scheme approximates the internal layers by means of jumps, while the IP schemes attempt to recover a numerical solution which is

Figure 1: Graphical comparison between the methods SWIP and IP-A. The test case with $\varepsilon_1 = $ 5e-2 is reported on the left while the case with $\varepsilon_1 = $ 5e-3 is on the right. In both cases $\varepsilon_2 = 1$. Each column shows the one-dimensional exact solution $u(x)$ of the test problem (top) and the numerical approximation u_h obtained with the methods SWIP (center) and IP-A (bottom), by means of piecewise-linear elements ($p = 1$). The case IP-B has been omitted since it is qualitatively equivalent to IP-A.
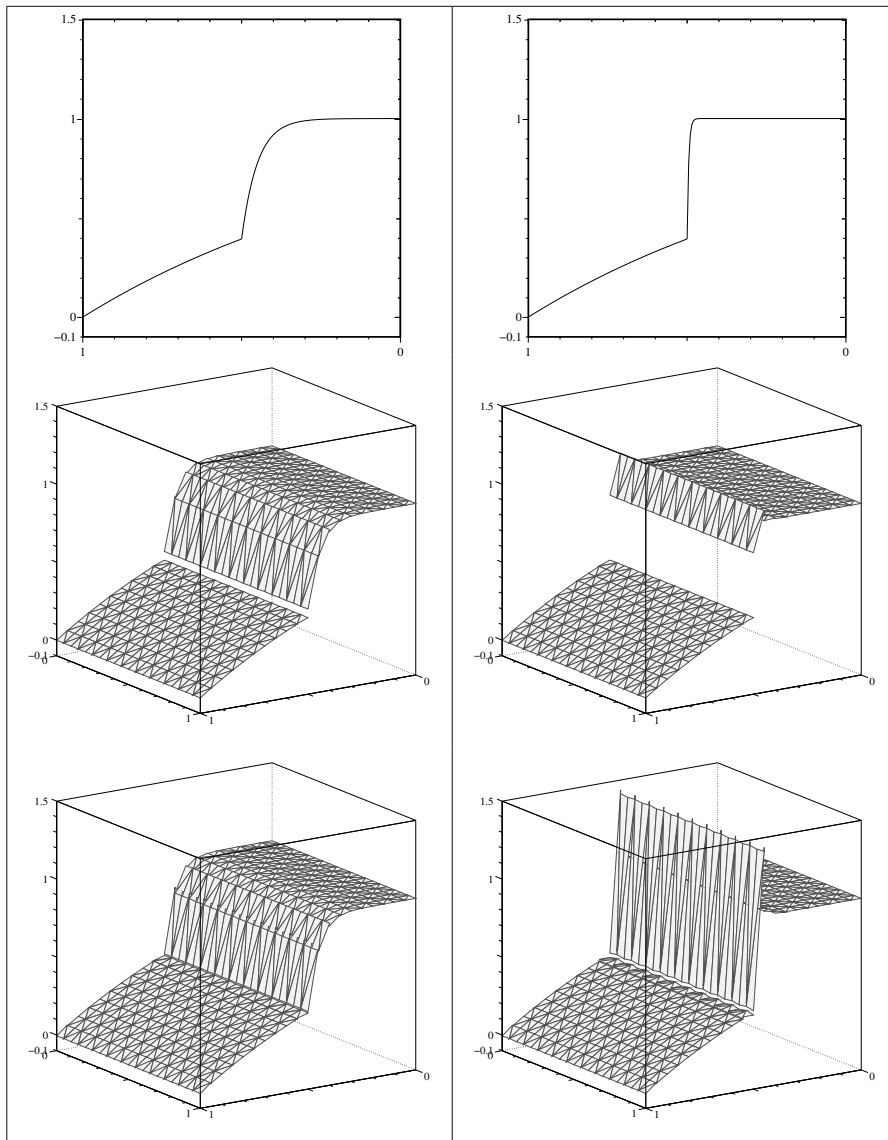
Figure 2: The norm $\|\cdot\|_{0,\Omega}$ and the indicator (49) (denoted by M) are plotted for the values $\varepsilon_1 = 2^{-i}$, $i = 0, \ldots, 16$. The methods SWIP, IP-A and IP-B are compared with respect to these indicators for linear (top) and quadratic elements (bottom).
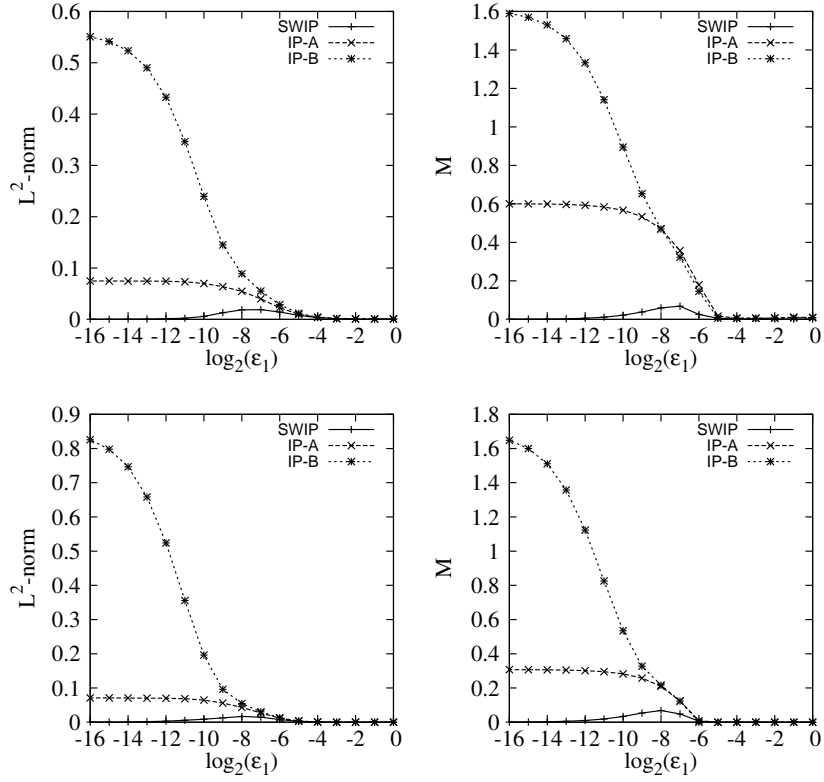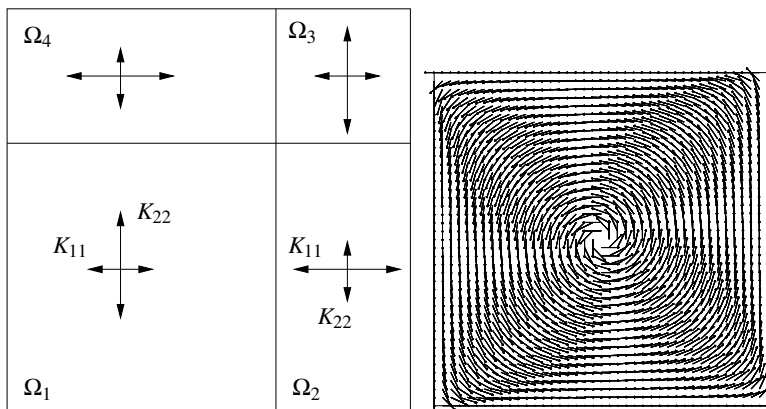

Figure 3: Test case with genuine anisotropic properties. On the left, an illustration of the domain and its subregions together with a synoptic description of the diffusivity tensor. The advection field β is shown on the right.

almost continuous. Since the computational mesh is insufficiently refined, the scheme IP-A generates some slight undershoots near the interfaces where K is discontinuous. For the IP-B method the oscillations generated by the approximation of the internal layer are much more evident and propagate quite far away from the interfaces. This behavior can be explained by observing that this type of penalty does not distinguish between the principal directions of the diffusivity tensor. Consequently, an excessive penalty is applied along the direction of low diffusivity.

To strengthen these conclusions, we also consider a numerical test where the advection field is the opposite of the one reported in Figure 3, i.e. it rotates clockwise. Following this advection field along the interfaces between subdomains, the diffusivity decreases. These conditions lead to an exact solution which is smooth in the neighborhood of the interfaces. In this case, the three methods are expected to behave similarly, as is confirmed by the numerical results reported in the right column of Figure 4.

6   Concluding remarks

The SWIP method analyzed in this paper is a DG method with weighted averages designed to approximate satisfactorily advection-diffusion equations with anisotropic and locally small diffusivity. A thorough a priori error analysis has been carried out, yielding robust and optimal error estimates that have been supported by numerical evidence. The SWIP method is an interesting alternative to other IP methods since it can approximate more sharply under-resolved internal layers caused by locally small diffusivity.

References

[1] D.N. Arnold. An interior penalty finite element method with discontinuous elements. *SIAM J. Numer. Anal.*, 19:742–760, 1982.

[2] G.A. Baker. Finite element methods for elliptic equations using nonconforming elements. *Math. Comp.*, 31(137):45–59, 1977.

[3] E. Burman and P. Zunino. A domain decomposition method based on weighted interior penalties for advection-diffusion-reaction problems. *SIAM Journal on Numerical Analysis*, 44(4):1612–1638, 2006.

[4] B. Cockburn and C.W. Shu. The local discontinuous Galerkin method for time-dependent convection-diffusion systems. *SIAM J. Numer. Anal.*, 35:2440–2463, 1998.

[5] J.-P. Croisille, A. Ern, T. Lelièvre, and J. Proft. Analysis and simulation of a coupled hyperbolic/parabolic model problem. *J. Numer. Math.*, 13(2):81–103, 2005.

[6] D.A. Di Pietro, A. Ern, and J.-L. Guermond. Discontinuous Galerkin methods for anisotropic diffusion with advection. *SIAM J. Numer. Anal.*, 2008. To appear.

Figure 4: Test case with genuine anisotropic properties. The advection field rotates counterclockwise on the left (see figure 3) and clockwise on the right. The solution obtained by the SWIP scheme is shown on the top while those relative to the IP-A and IP-B methods are depicted below.
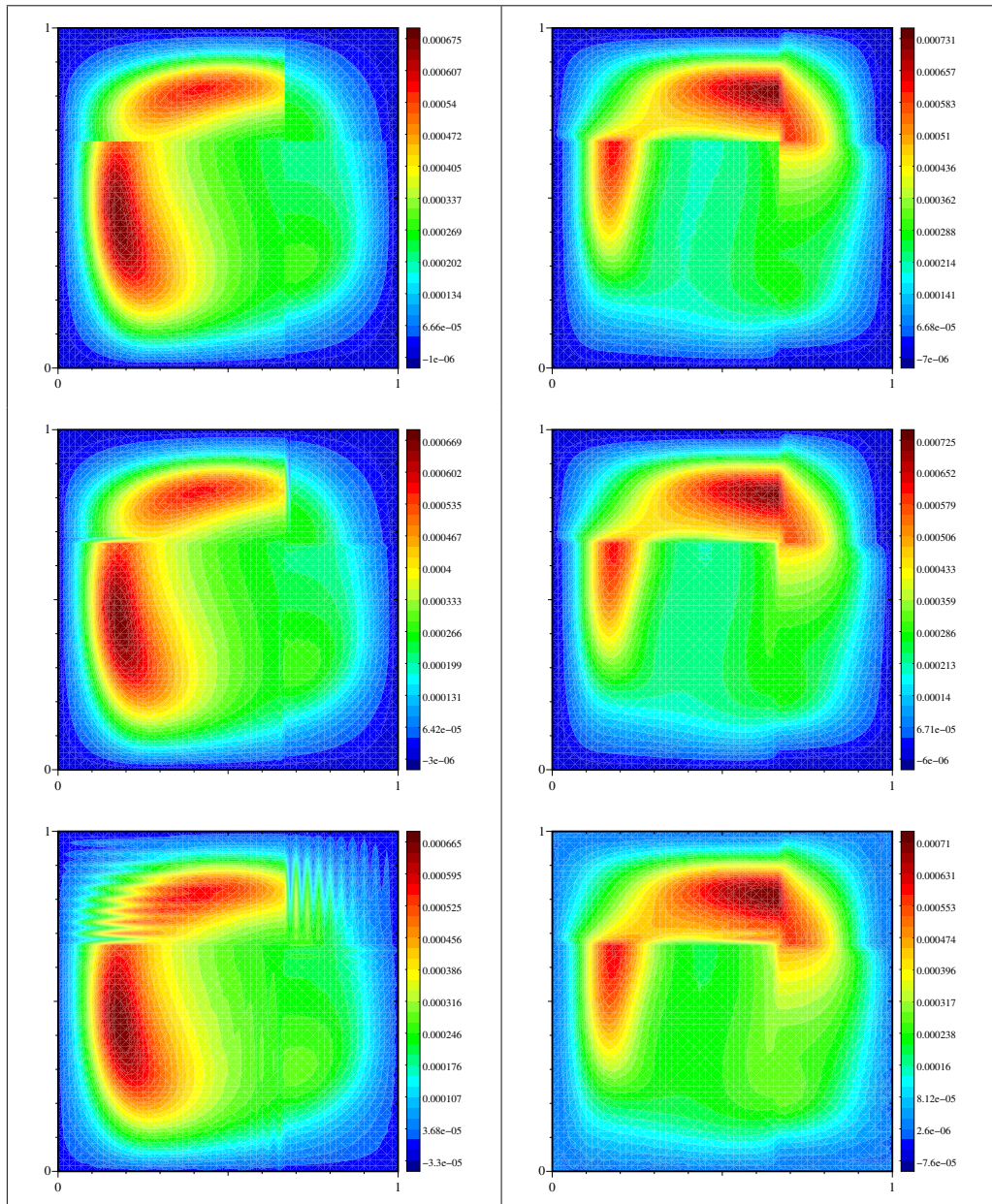
[7] A. Ern and J.-L. Guermond. Discontinuous Galerkin methods for Friedrichs' systems. I. General theory. *SIAM J. Numer. Anal.*, 44(2):753–778, 2006.

[8] A. Ern and J. Proft. Multi-algorithmic methods for coupled hyperbolic-parabolic problems. *Int. J. Numer. Anal. Model.*, 1(3):94–114, 2006.

[9] Alexandre Ern and Jean-Luc Guermond. *Theory and practice of finite elements*, volume 159 of *Applied Mathematical Sciences*. Springer-Verlag, New York, 2004.

[10] F. Gastaldi and A. Quarteroni. On the coupling of hyperbolic and parabolic systems: analytical and numerical approach. *Appl. Numer. Math.*, 6(1-2):3–31, 1989/90. Spectral multi-domain methods (Paris, 1988).

[11] Emmanuil H. Georgoulis and Andris Lasis. A note on the design of hp-version interior penalty discontinuous Galerkin finite element methods for degenerate problems. *IMA J. Numer. Anal.*, 26(2):381–390, 2006.

[12] B. Heinrich and S. Nicaise. The Nitsche mortar finite-element method for transmission problems with singularities. *IMA J. Numer. Anal.*, 23(2):331–358, 2003.

[13] B. Heinrich and K. Pietsch. Nitsche type mortaring for some elliptic problem with corner singularities. *Computing*, 68(3):217–238, 2002.

[14] B. Heinrich and K. Pönitz. Nitsche type mortaring for singularly perturbed reaction-diffusion problems. *Computing*, 75(4):257–279, 2005.

[15] P. Houston, Ch. Schwab, and E. Süli. Discontinuous hp-finite element methods for advection-diffusion-reaction problems. *SIAM J. Numer. Anal.*, 39(6):2133–2163, 2002.

[16] P. Lesaint and P.-A. Raviart. On a finite element method for solving the neutron transport equation. In C. de Boor, editor, *Mathematical aspects of finite elements in partial differential equations (Proc. Sympos., Math. Res. Center, Univ. Wisconsin, Madison, Wis., 1974)*, pages 89–123. Publication No. 33. Math. Res. Center, Univ. of Wisconsin-Madison, Academic Press, New York, 1974.

[17] J. Nitsche. Über ein Variationsprinzip zur Lösung von Dirichlet-Problemen bei Verwendung von Teilräumen, die keinen Randbedingungen unterworfen sind. *Abh. Math. Sem. Univ. Hamburg*, 36:9–15, 1971. Collection of articles dedicated to Lothar Collatz on his sixtieth birthday.

[18] J. Nitsche. On Dirichlet problems using subspaces with nearly zero boundary conditions. In A. K. Aziz, editor, *The mathematical foundations of the finite element method with applications to partial differential equations*, pages 603–627. Academic Press, New York, 1972.

[19] W.H. Reed and T.R. Hill. Triangular mesh methods for the neutron transport equation. Technical Report LA-UR-73-479, Los Alamos Scientific Laboratory, Los Alamos, NM, 1973.

[20] B. Rivière, M. Wheeler, and V. Girault. Improved energy estimates for interior penalty, constrained and discontinuous Galerkin methods for elliptic problems. Part I. *Comput. Geosci.*, 3:337–360, 1999.

[21] R. Stenberg. Mortaring by a method of J.A. Nitsche. In Idelsohn S.R., Oñate E., and Dvorkin E.N., editors, *Computational Mechanics: New trends and applications*, pages 1–6, Barcelona, Spain, 1998. Centro Internacional de Métodos Numéricos en Ingeniería.